

Analysis of Polarization Responses According to Different Land Cover Types Using SAR Polarimetry Data

M. K. Kang

Chonnam National University
300 Yongbong-dong Buk-gu, Gwangju 500-757, Korea
heidiyaa@lycos.co.kr

W. J. Yoon

Chonnam National University
300 Yongbong-dong Buk-gu, Gwangju 500-757, Korea
wjyoon@chonnam.ac.kr

K. E. Kim

Korea Institute of Geoscience & Mineral Resources
30 Kajung-dong Yusung-gu, Daejeon 305-350, Korea
kimke@rock25t.kigam.re.kr

H. S. Choi

Chonnam National University
300 Yongbong-dong Buk-gu, Gwangju 500-757, Korea
ggumikni@freechal.com

Abstract: In this paper, multifrequency, polarimetric SAR data acquired during the first SIR-C/XSAR mission over the Seoul and Gyunggi-do (Korea) test sites are analyzed. The main objective of the study is to assess the possibility of extracting relevant information about surface properties for geophysical applications using polarimetry. This study analyses the characteristics of polarization responses and polarimetric parameters to conditions present in urban, river, agricultural, and forested areas. Results indicate that the dominant scattering property from these fields varies depending on the land cover types. The polarization response graphs and the backscattering coefficients associated with the polarimetric parameters are also useful in characterizing these cover types.

Keywords: SAR polarimetry, SAR.

1. Introduction

Radar polarimetry is concerned with control of polarimetric properties (electric field direction behavior) of radar waves and the extraction of target properties from the behavior of scattered (reflected) waves from a target [1]. Many radar targets are inherently polarimetric, and vector control of the transmitted wave and complete polarimetric reception of the scattered wave are essential in determining the target characteristics.

A particular graphical representation of the variation of scattering cross section as a function of polarization, known as the polarization signature or polarization response, is quite useful for describing polarization properties of point and distributed targets. The response consists of a plot of synthesized scattering cross section as a function of the ellipticity and orientation angles of the transmitted wave [2]. In the case of co-polarized responses, the transmitting and receiving antennas have the

same polarization; in the case of the cross-polarized responses, the receiving antenna is polarized orthogonally to the transmitting antenna.

Some targets that can be polarimetrically identified include urban areas whose polarimetric microwave scattering from radars is characteristic of double reflections from ground to buildings and back to the radar, forested area whose reflections have large randomly-directed components, and ocean areas with polarimetric scattering properties strongly dependent on sea states. Other radar target properties that are polarimetric include oil spill thickness, rainfall rates and drop size, crop health, and ground moisture content.

The objective of this study is to investigate a physically based interpretation of observed polarimetric radar responses according to different land cover types. The co-polarized and cross-polarized response graphs and polarimetric parameters are discussed.

2. Data and Image Processing

1) SIR-C Image Data and Land Classification Data

The SAR data analyzed in this study are multi look complex (MLC) images acquired by the fully polarized SIR-C system over Seoul and Gyunggi-do (Korea) on April 12, 1994. SIR-C acquisition mode was fully polarimetric at C (5.304 GHz) and L (1.254 GHz) band and the orbit direction was descending.

Land classification data used in this work was supplied by the Ministry of Environment Republic of Korea (MOE) and was made by image fusion method using Landsat TM and IRS-1C Pan images acquired in May, 1999 and February, 2000.

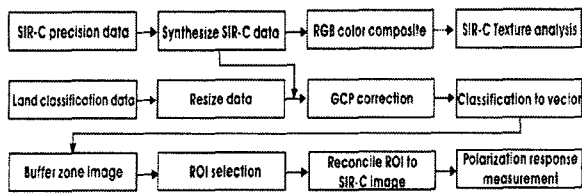


Fig. 1. Schematic diagram of image processing for polarization responses measurement.

2) Image Processing

SIR-C MLC images were synthesized HH, VV, HV polarizations and total power (TP) images from SIR-C compressed scattering matrix. And then the HH, VV, and HV polarization images as RGB were synthesized. Land classification data were resized corresponding to SIR-C coverage and was georeferenced to the SIR-C image. Four categories of land cover types were chosen for polarization response measurement of SAR data. Four major types of land cover are discriminated: urban, river, agricultural, and forested areas. In this study, two kinds of polarization responses of co- and cross-polarized were measured according to different land cover types which were urban, river, agricultural (rice, and ordinary), and forested (broadleaved, coniferous, and mixed) regions. The results measured at respective areas are compared with theoretical polarization response graphs of several representative reflectors. The SIR-C data was processed by JPL, which provides multi look compressed data. From the delivered data, the following quantities are calculated for each frequency: the backscattering coefficients σ_{HH}^0 , σ_{VV}^0 , and σ_{HV}^0 (for the HH, VV, and HV polarizations, respectively), the co-polarized $\sigma_{HH}^0 / \sigma_{VV}^0$ ratio and the cross-polarized $\sigma_{HH}^0 / \sigma_{HV}^0$ ratio.

3. Results

1) SIR-C Image Texture Analysis

A useful rule-of-thumb in analyzing radar images is that the higher or brighter backscatter on the image. Flat surfaces that reflect little or no microwave energy back towards the radar will always appear dark in radar images. Vegetation is usually moderately rough on the scale of most radar wavelengths and appears as grey or light grey in a radar image. Surfaces inclined towards the radar will have a stronger backscatter than surfaces which slope away from the radar and will tend to appear brighter in a radar image. Some areas not illuminated by the radar, like the back slope of mountains, are in shadow, and will appear dark. When city streets or buildings are lined up in such a way that the incoming radar pulses are able to bounce off the streets and then bounce again off the buildings (called a double-bounce) and directly back towards the radar they appear very bright in radar images. Roads and freeways are flat surfaces so appear dark. Buildings which do not line up so that the radar pulses are reflected straight back will appear light

grey, like very rough surfaces.

Fig.2 and Fig. 3 display the imagery of RGB color composites of three channels HH, VV, and HV for each frequency. SAR texture analysis may provide additional information for a better discrimination of polarimetric properties of surface elements. Red, Green, and blue color appear at regions observed HH, VV, and HV polarizations dominantly. Yellow areas are very strong and are recorded as bright signals in co-polarized (HH and VV).

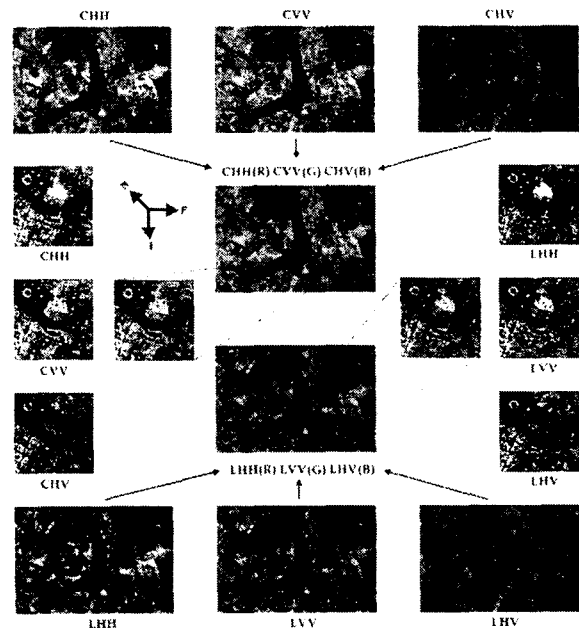


Fig. 2. SIR-C RGB (HH, VV, HV as RGB) color composite images for urban texture appeared mainly.

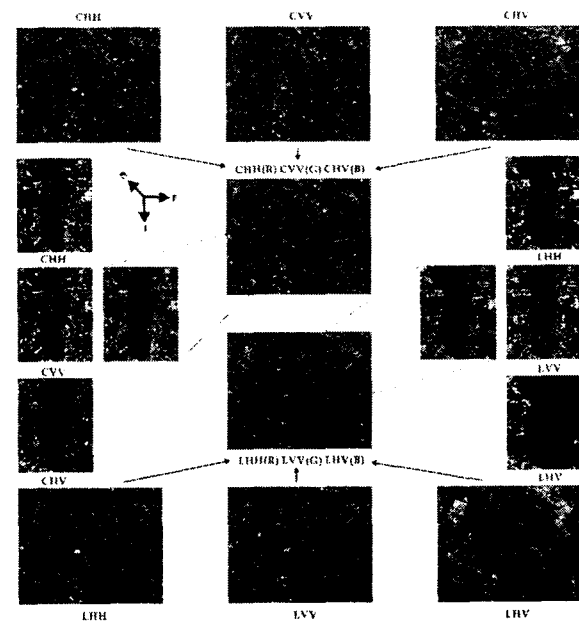


Fig. 3. SIR-C RGB (HH, VV, HV as RGB) color composite images for agricultural texture appeared mainly.

2) Polarization Response Behavior

Three dimensional polarization response graphs are commonly used in the literature to illustrate the polarimetric properties of terrain elements. These graphs display the properties of co- or cross-polarized polarimetric radar returns as they are distributed over half of Poincaré sphere. In general, the signatures should show systematic variation with incident angle for specific material types and should identify preferred polarization states for material classification where these exist [1].

C and L band polarization responses measured according to chosen land cover types show the results that the polarization behavior for large a conducting sphere appears in river, agricultural, and forested areas, and the polarization behavior for a dihedral corner reflector or a short, thin cylinder reflector appears in the urban area. Fig. 4 displays the measured co- and cross-polarized responses for C and L band in urban areas. The polarization characteristics of the urban area show the behaviors for the thin cylinder or dihedral corner reflector unlike the other areas, because of double reflections from ground to buildings and back to the radar.

In general, a wave scattered from a dihedral corner reflector will undergo a reflection at each surface and return in the direction from which it came. The co- and cross-polarized responses of the dihedral corner reflector are very different from those of the sphere. The co-polarized response possesses two minima at linear polarizations offset by $\pm 45^\circ$ from the horizontal and vertical polarizations, and the cross-polarized response has maxima at these locations [2]. For the cylinder oriented, the maximum in the co-polarized response and one of the minima in the cross-polarized response occur at the linear polarization with the same orientation as the cylinder. Both the co-polarized and cross-polarized responses also have minima at the linear polarization orthogonal to the cylinder orientation.

Fig. 5, Fig. 6, and Fig. 7 show polarization response graphs of river, agricultural, and forested areas. Co- and cross-polarized responses were measured from 34, 23, 17, 15, 10, and 14 ROIs in river, rice, and ordinary agricultural, broadleaved, coniferous, and mixed forested areas respectively. Agricultural areas were selected rice (agri_1) and ordinary (agri_2) agricultural fields corresponding to land classification data. Broadleaved, coniferous, and mixed forested areas were described forest_1, forest_2, and forest_3. The results of river, agricultural, and forested areas show the polarization behavior of a flat surface or a large conducting sphere characteristics.

For a large conducting sphere, the co-polarized response shows that the maximum measured scattering cross section occurs for linear polarizations and the scattering cross section is independent of the linear polarization orientation angle. This independence is a consequence of the lack of preferred orientation for a sphere. For the cross-polarized response, the measured scattering cross section is greatest for the circular polarizations and

smallest for linear polarizations. The maxima occur at the circular polarizations because the scattered waves for circularly polarized incident waves are also circularly polarized, but with the opposite sense of rotation. A large flat surface at normal incidence would have the same polarization responses as a large sphere.

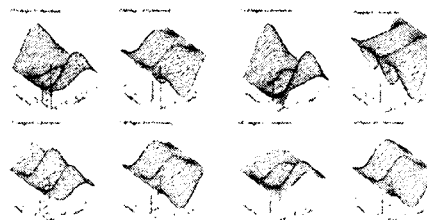


Fig. 4. Co-polarized (1st, 3rd) and cross-polarized (2nd, 4th) responses for C band (1st, 2nd) and L band (3rd, 4th) in urban areas (#1, #10).

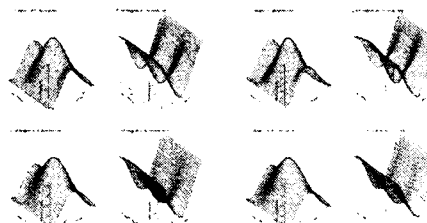


Fig. 5. Co-polarized (1st, 3rd) and cross-polarized (2nd, 4th) responses for C band (1st, 2nd) and L band (3rd, 4th) in river areas (#7, #16).

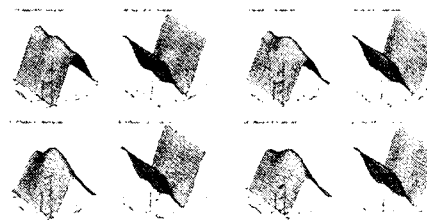


Fig. 6. Co-polarized (1st, 3rd) and cross-polarized (2nd, 4th) responses for C band (1st, 2nd) and L band (3rd, 4th) in agricultural areas (agri_1 #10, agri_2 #12).

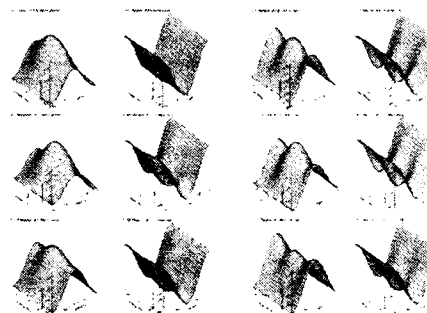


Fig. 7. Co-polarized (1st, 3rd) and cross-polarized (2nd, 4th) responses for C band (1st, 2nd) and L band (3rd, 4th) in forested areas (forest_1 #3, forest_2 #1, forest_3 #1).

Table 1. Radar characteristics of training sites for land cover type classes at C and L band frequencies.

Class	Avg σ_{HH}^o	Std σ_{HH}^o	Avg σ_{VV}^o	Std σ_{VV}^o	Avg σ_{HV}^o	Std σ_{HV}^o	ROIs
C band (1st row: co-polarized, 2nd row: cross-polarized)							
Urban	1.4812	1.2127	0.8830	0.4356	0.0644	0.0190	28
	2.8781	2.3718	1.7028	0.7666	0.1259	0.0370	
River	0.0197	0.0066	0.0292	0.0098	0.0008	0.0003	34
	0.0338	0.0118	0.0497	0.0162	0.0013	0.0006	
Agri_1	0.2675	0.0662	0.2585	0.0675	0.0320	0.0053	23
	0.3576	0.0849	0.3445	0.0809	0.0429	0.0060	
Agri_2	0.2523	0.1536	0.2444	0.1279	0.0232	0.0119	17
	0.3522	0.1869	0.3415	0.1519	0.0327	0.0148	
For-est_1	0.2000	0.0346	0.2346	0.0370	0.0419	0.0072	15
	0.3209	0.0521	0.3766	0.0574	0.0672	0.0108	
For-est_2	0.1674	0.0402	0.1957	0.0517	0.0331	0.0080	10
	0.2694	0.0563	0.3161	0.0788	0.0537	0.0133	
For-est_3	0.1867	0.0625	0.2142	0.0608	0.0381	0.0124	14
	0.2959	0.0908	0.3401	0.0878	0.0604	0.0184	
L band (1st row: co-polarized, 2nd row: cross-polarized)							
Urban	0.7455	0.6607	0.4364	0.1857	0.0272	0.0080	28
	1.5319	1.3985	0.8784	0.3856	0.0536	0.0139	
River	0.0159	0.0052	0.0287	0.0110	0.0008	0.0003	34
	0.0270	0.0104	0.0482	0.0180	0.0013	0.0004	
Agri_1	0.1225	0.0614	0.1218	0.0532	0.0096	0.0036	23
	0.1624	0.0801	0.1607	0.0646	0.0128	0.0052	
Agri_2	0.1116	0.1001	0.1046	0.0629	0.0081	0.0063	17
	0.1616	0.1517	0.1504	0.0941	0.0118	0.0098	
For-est_1	0.1729	0.0386	0.1731	0.0309	0.0265	0.0058	15
	0.2642	0.0533	0.2646	0.0406	0.0406	0.0085	
For-est_2	0.1759	0.0748	0.1630	0.0540	0.0245	0.0089	10
	0.2771	0.1358	0.2546	0.0940	0.0382	0.0147	
For-est_3	0.1732	0.0675	0.1575	0.0537	0.0254	0.0111	14
	0.2713	0.1036	0.2465	0.0811	0.0398	0.0170	

Table 1 lists the radar backscatter characteristics for the chosen training areas. σ_{HH}^o , σ_{VV}^o , and σ_{HV}^o are the SIR-C backscattering coefficients in normalized over training areas. Avg and Std stand for the mean and standard deviation.

3) HH/VV Ratio vs. HH/HV Ratio

Fig. 8 and Fig. 9 show HH/VV ratio (normalized) versus HH/HV ratio (normalized) including all the measurement data sets at C and L bands. The results of the scatter plot of HH/VV ratio versus HH/HV ratio measured from different land cover types show that urban areas appear a positive relation and the river, agricultural, and forested areas are less linearly related. However, it appears to be a good candidate for the discrimination between surface and volume scattering of land cover characteristics.

4. Conclusions

The objective of this work has been to assess the use of polarimetric SAR data in order to extract relevant information about land surface properties for geophysical applications. Analysis of fully polarimetric SAR data is an interesting and important way to characterize the scattering behavior of many targets.

Results of polarization responses and polarimetric parameters indicate that the dominant scattering property from these fields varies depending on the land cover type. Polarization response graphs show that polarization behavior for large a conducting sphere appears at river, agriculture, and forest areas, and the polarization behavior for a dihedral corner reflector or a short, thin cylinder

reflector appears in the urban area. The polarization response graphs and backscattering coefficients associated with the polarimetric parameters, especially co-polarized HH/VV ratio and cross-polarized HH/HV ratio are useful in characterizing these surface types.

References

- [1] Henderson, F. M., Lewis, A. J. (eds.), 1998. *Principles & Applications of Imaging Radar*, John Wiley & Sons, NY.
- [2] Ulaby, F. T., Elachi, C. (eds.), 1990. *Radar Polarimetry for Geoscience Application*, Artech House.
- [3] Elachi, C., 1998. *Spaceborne Radar Remote Sensing: Applications and Techniques*, IEEE Press, NY

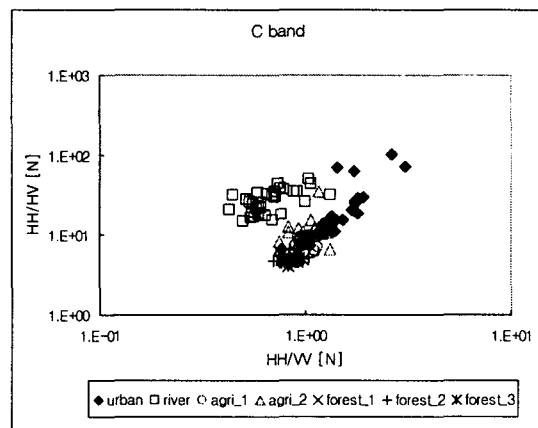


Fig. 8. Plot of HH/VV ratio versus HH/HV ratio (Normalized) for C band.

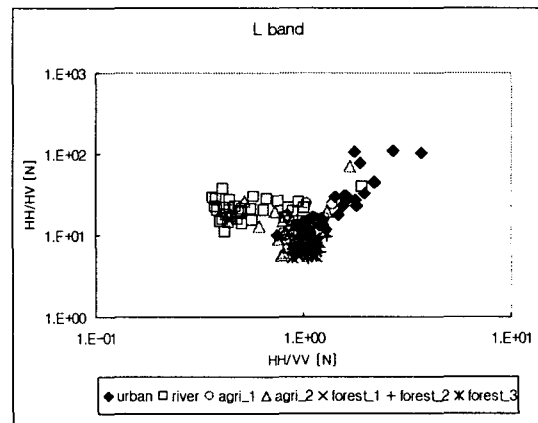


Fig. 9. Plot of HH/VV ratio versus HH/HV ratio (Normalized) for L band.